J Exp Neurol. 2022;3(2):24-34.

Journal of Experimental Neurology Research Article

A Rodent Lumbosacral Spinal Cord Injury Model Reflecting Neurological and Urological Deficits of Humans

Behnaz Afrashteh[1,2,3], Karin Roider[1,2,3], Sophina Bauer[1,2,3], Lukas Lusuardi[3], Patrick Heimel[4,5,6], David Hercher[5,6], Ludwig Aigner[1,2], Esra Keller[1,2,3*]

[1]Institute of Molecular Regenerative Medicine, Paracelsus Medical University Salzburg, Austria

[2]Spinal Cord Injury and Tissue Regeneration Center, Paracelsus Medical University Salzburg, Austria

[3]Department of Urology, University Clinic, Paracelsus Medical University, Salzburg, Austria

[4]Karl Donath Laboratory for Hard Tissue and Biomaterial Research, University Clinic of Dentistry, Medical University Vienna, Austria

[5]Ludwig Boltzmann Institute for Traumatology, Vienna, Austria

[6]Austrian Cluster for Tissue Regeneration, Vienna, Austria

[*]Correspondence should be addressed to Dr. Elena Esra Keller, esra.keller@pmu.ac.at

Received date: March 18, 2022, **Accepted date:** April 27, 2022

Citation: Afrashteh B, Roider K, Bauer S, Lusuardi L, Heimel P, Hercher D, et al. A Rodent Lumbosacral Spinal Cord Injury Model Reflecting Neurological and Urological Deficits of Humans. J Exp Neurol. 2022;3(2):24-34.

Abstract

Spinal cord injury (SCI) to the terminal segments of the spinal cord causes severe disruption of the neural circuitry of the bladder, resulting in neurogenic underactive bladder (nUAB). We developed a rodent lumbosacral injury model to investigate the effects of bladder function and structure. A severe contusion SCI was performed over the L5-S2 segmental spinal cord (T13/L1 junction, L1 vertebra, L1/L2 junction). The injured spinal cords were scanned by advanced micro-CT imaging. Bladder function was assessed in awake rats before and at 2, 4, 6, and 8 weeks after SCI. Locomotor function was assessed using the BBB Open Field Rating Scale and the Catwalk system. Specific histological staining assessed structural bladder remodelling in control and SCI rats. Contusion SCI at the three respective segmental heights revealed variations in lesion sizes and white and gray matter sparing. However, this did not influence SCI rats' bladder and locomotor outcomes, whereas the functional deficits were comparable in control and SCI rats. From week 2 onwards, the main functional changes of nUAB in SCI rats were noticeable: a low detrusor strength with a combination of slow maximal flow rate and low leakage volumes with no to incomplete voiding. Histological analyses of bladder tissue underlined the functional outcomes by depicting a thickened bladder wall with ongoing fibrotic and uroepithelial changes. As expected, only mild locomotor impairments were determined. This model of lumbosacral SCI reproduces nUAB with structural and functional outcomes similar to human nUAB, giving future studies a well-defined framework to test therapies for nUAB conditions in a standardized rat model.

Keywords: Rat model; Lumbosacral level; Underactive bladder; Spinal cord injury; Neurogenic bladder

Introduction

Traumatic spinal cord injury (SCI) is a serious combat-related injury that is becoming increasingly common in modern warfare [1]. The urinary system is considered particularly vulnerable in patients with such neurological conditions, and renal failure due to bladder filling and voiding dysfunction and chronic urinary tract infections are the leading causes of second hospitalization in these patients [2,3]. Therefore, the initial diagnosis of urinary tract dysfunction is critical for counselling patients, setting rehabilitation goals, and determining an intervention tailored to the patient. Based on the fact that bladder function is steered by interacting motoneurons at T12-L1 (in spinal cord segments S2-S4) and higher brain centers, for lesions above T12, the terms "upper motor neuron lesion" (overactive detrusor with a contractile urinary sphincter) and below T12 "lower motor neuron lesion" (areflexia with paralysis of the urinary sphincter) have been used [4-6].

In the case of damage below the T12 spine, some or all of the nerves in this region are affected, depending on the type of lesion. If all nerve roots are affected, there will be an acontractile detrusor and sphincter. However, because the spinal cord terminates at approximately L2, a lesion at the thoracolumbar junction and at the L1 spine would result in different clinical features [7,8].

Interestingly, however, in recent studies reporting on the development of new models of SCI at the lumbar level in rodents by peripheral nerve crush [7], ventral root avulsion (VRA) [9] and lumbar canal stenosis (LCS) [10], unlike the denervated EUS muscle that becomes flaccid [11], the bladder may maintain reinnervation with improvement in voiding efficiency. This is in contrast to the situation in humans, because most of SCIs at this level are incomplete and caused by fractures with permanent damage to the bladder reflex segment in the spinal cord.

Accordingly, the present study aimed to directly assess whether there were differences in bladder dysfunction following contusive SCI at T13/L1 junction, L1 vertebral level and L1/L2 junction in a rat model. We report here that histologically all different lesions at segments L5-S2 produced severe changes in the structure and function of the bladder, whereas the locomotor function was mildly impaired.

Materials and Methods

Animals and study protocol

A total of 20 adults (190–230 g) female Lewis rats (strain LEV/Crl, Charles River) were studied. Rats were group- housed at controlled temperature, humidity, and light cycle. All experimental procedures conformed with the Austrian Law on the Protection of Animals. The animals were divided into two groups: neurologically intact rats (intact group, n = 4) and SCI group with severe contusion at T13/L1 junction (SCI, n = 4), L1 vertebral level (SCI, N=4) and L1/L2 junction (SCI, n=4). Due to a technical error, four animals received an injury not in the interest areas. We have excluded data from these animals due to the outlier status.

Surgical procedures

Catheter implantation: For a detailed implantation protocol, please refer to the following publications [12,13].

In brief, under general anaesthesia (medetomidine hydrochloride (Narcostart 1 mg/ml), midazolam (5 mg/ml) and Fentanyl-Janssen (0.1 mg/ml), based on the body weight of the individual animal), a PE-50 bladder catheter was implanted via the bladder dome into the bladder. The bladder catheter was tunnelled subcutaneously and exteriorized at the level of the scapulae. Analgesic and antibiotic coverage (Metacam 0.05 mg/kg and Baytril 5 mg/kg) were administered for five post-surgical days.

Spinal cord injury: In general anaesthesia (details, see above) a standard laminectomy was performed at the T13/L1 level. An IH-0400 infinite horizon impactor (Precision Systems & Instrumentation, Fairfax Station, VA) was used to apply a dorsal-ventral impact with a force of 300 kDyne. Analgesic and antibiotic coverage was given as outlined above. Follow up period post SCI was 8 weeks.

Functional analysis

Evaluation of bladder function: Awake urodynamic was done as described in detail elsewhere [12,13] once prior to SCI and after that weekly. Room-temperature warm saline solution was instilled via the catheter line into the bladder at a speed of 120 µl/min. The intravesical pressure (Pves) and voided volume (VV) events were recorded for 60 minutes at a sampling rate of 60 Hz using pressure and force transducer, respectively (World Precision Instruments. Sarasota, FL). Cystometric data were acquired and analysed using catamount software (Med Associates, CAT-CYT-M).

Evaluation of locomotor behaviors: Two condition-blind observers evaluated Open-field locomotion before surgery; and at 1, 16, 29, 43, and 55 d post-surgery using the 21-point BBB locomotion scale [14]. Gait analyses of voluntary locomotion were performed using the Catwalk XT system for rats with BBB scores of 11 or higher. Every session consisted of six good runs defined as transit across the recording window with a variation of the walking speed of less than 60%. Each paw was documented and compared using a nonparametric test for longitudinal data. Since the lesions are bilateral and ratio of left hind limb to right hind limb is 1, for comparison of the experimental groups, only the ratio of left hind limb post SCI to pre-SCI was measured for analyses. The parameters were print area, base of support and swing time.

In- vitro experiments

Tissue harvesting and assessments: Eight weeks after SCI, the rats were deeply IV anesthetized via intraperitoneal injection of ketamine (273 mg/kg), Xylazine (7.1 mg/kg), and Acepromazine (0.625 mg/kg). They were transcardially perfused via the aorta with heparinized saline solution (slow steady drip (20 ml/min)) followed by ice-cold 4% paraformaldehyde solution (20 ml/min).

Histological staining: For histological analysis, the bladders were embedded in paraffin. The paraffin blocks were transversely cut into 10 µm serial sections and documented by a Slide Scanner (Leica SCN400) microscope. The contents of urothelial, connective, smooth muscle and vascular tissue by Masson-Goldner trichrome and collagen type I and III by Herovici staining were quantified by means of ImageJ analysis software (National Institutes of Health, Bethesda, MD, USA). For elastic fiber quality, Orcein stained sections, were documented by an Olympus CX23 microscope at 63x.

Contrast agent-enhanced µCT scan: Following perfusion (see above), the excised spinal cords were stained by submersion in contrast agent Accupaque-350 (GE Healthcare, Munich, Germany) diluted 1:2 in PBS for 48 h and scanned in a SCANCO µCT 50. Spinal cords were mounted on 2*4 mm strips of XPS board attached by gently wrapping ~ 5 mm wide strips of parafilm gently around the spinal cords above and below the defect region. Scans were performed at 70 kVp with 85 µA using a 0.5 mm Al Filter. 1250 Projections/180° were integrated 2 times for 750 ms and averaged. The scans were reconstructed to an isotropic resolution of 6 µm. Approximately 16 mm of spinal length was scanned centered on the epicenter of the lesion. Volume of interest (VOI) was analyzed semi-automatically using Fiji (ImageJ v1.53a) [15] with a newly developed algorithm. The outer border of white matter, gray matter and damaged regions were manually marked using the ROI manager and interpolation. The cyst was segmented using a threshold adjusted to the density of the pure contrast agent in each image. The primary readout parameters remained white and gray matter compared to healthy reference, cyst size and cyst distribution.

Statistical analysis

Standard tests were used to check the data of the individual urodynamic measurements (intravesical pressure, filling volume, bladder compliance and micturition behavior) on the normal distribution and variance homogeneity. For time-course data, a repeated measures two-way ANOVA was used. In addition, a parametric unpaired one-way ANOVA and t-test were used for data analyzed at a single time point which provided the statistically significant differences between the parameters before and after SCI. Standard software packages (e.g. GraphPad Prism 9) were used for the calculations. Data were significant when $p<0.05$. Data were plotted as the mean ± SEM.

Results

The spinal cord lesion areas were characterized by Micro CT scanning

In a first step, by using an advanced µCT imaging, we determined (i) the location, size and severity of the lesions, and (ii) the sparing of white and gray matter at the epicenter, 8 weeks post-SCI. The SCI rats were classified into three distinct groups according to the neuropathological damage from vertebral levels. Group A included SCI at the thoracolumbar junction with a segmental lesion area ranging from mid L5 to mid L6 and bilateral dorsoventrally epicenter damage, (group B) vertebral L1 with segmental lesion area ranging from mid L6 to mid S1 and bilateral dorsal and unilateral ventral, and (group C) L1/L2 junction with segmental lesion area stretching from the beginning S1 to one third S2 and bilateral dorsoventrally epicenter damage (Figure 1A, b). Lesion length, lesion volume, cyst volume and spared white and gray matter

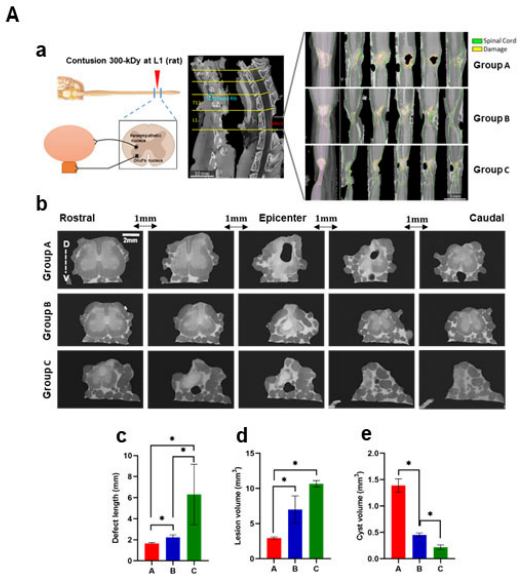

Figure 1A: **(a)** Dorsal view of spinal cords 8 weeks post SCI visualized by µCT scanning. The µCT imaging showing the laminectomy at L1 vertebral canal. µCT projection along the dorsoventral axis, blue lines indicate the position of the five equidistant curved slices, showing the variations of the lesion levels along the rostro-caudal axis. (Group A) Lesion area, rostral to caudal, from mid L5 to mid L6. (Group B) Lesion area from mid L6 to mid S1. (Group C) Lesion area from beginning S1 to one third of S2. **(b)** Cross sections of the lesion area, 1 mm cranial and caudal from the epicenter. Bar graphs represent **(c)** the defect length along the spinal cord, **(d)** the lesion volume (mm^3), based on the defect length (mm) × epicenter area (mm^2), **(e)** cyst volume (mm3). Data represent mean ± S.E.M. n = 4/group. $P<0.05$ indicates statistical significance difference. *$p < 0.05$. The significance difference was evaluated by One-way ANOVA. Magnification 20x. R: Rostral; C: Caudal; V: Ventral; D: Dorsal; E: Epicenter.

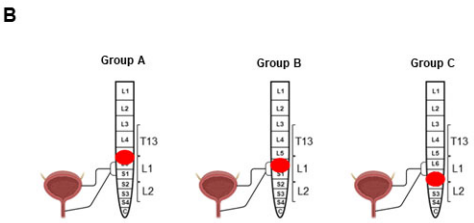

Figure 1B: Areas of spinal cord damage produced by lumbosacral contusion SCI. Group A: Destruction of T13/L1 junction. Group B: Destruction of L1 and surrounding lumbar roots. Group C: Destruction of L1/L2 junction with peripheral nerves.

Table 1: Values of interest in the lesion area.

Parameter	Group A	Group B	Group C	P-Value
Defect length (mm)	1.65 ± 0.09	2.24 ± 0.23	6.3 ± 2.88	0.1499
Lesion volume (mm^3)	2.94 ± 0,14	7± 1.93	10.66 ± 0.44	0.0771
Cyst volume (mm^3)	1.4 ± 0.12	0.45 ± 0.03	0.22 ± 0.04	0.0036
Sham White Matter (%)	69.27 ± 2.7	64.25 ± 0.14	65.22 ± 5.1	0.5505
Minimum White Matter (%)	6.35 ± 1.62	4.79 ± 0.02	0	0.0025
Sham Gray Matter (%)	30.73 ± 2.7	35.7 ± 0.18	34.78 ± 5.1	0.5567
Minimum Gray Matter (%)	0.31	0	0	-
Sham White Matter		Spared White matter at the same level of epicenter in lesion area in sham		
Sham Gray Matter		Spared Gray matter at the same level of epicenter in lesion area in sham		
Minimum White Matter		Spared White Matter at epicenter of lesion area (least percentage of Gray Matter)		
Minimum Gray Matter		Spared Gray Matter at epicenter of lesion area (least percentage of Gray Matter)		

n=4/group. Values are presented as mean ± SEM. P< 0.05 indicates statistical significance difference. P-value represents the significance difference among SCI group means (Two-way ANOVA).

are shown in graphs b-c and Table 1. The lesion pattern from rostral to caudal showed continual increases in defect length and lesion volume (Figures 1A, c-d). Cystic cavities surrounded by rims of anatomically preserved white matter were observed in all three groups, with group B depicting the largest cysts (average amount:1,4 mm^3, Figure 1, A e).

Lumbosacral SCI caused detrusor underactivity with high compliance

Bladder function was evaluated by awake repetitive measurements healthy and SCI rats. Table 2 shows the influence of lumbosacral SCI on defined urodynamic parameters. Most striking was that in all recordings functional deficits were identical, irrespective of the injury group and severity. Lumbosacral SCI resulted in significant reductions in maximum intravesical pressures (Figure 2b). While mean maximum intravesical pressure ranged 38,1 ± 6,28 cmH_2O pre SCI, it continuously dropped to average 12,04 ± 1,69 cmH_2O at 8 weeks post-SCI (Figure 2c). Threshold pressure to trigger micturition pre-SCI was 14,93 ± 2,97 cmH_2O and pointedly decreased after SCI (Figure 2e). Present low leaking volumes post SCI are shown in Figure 2d. Low intravesical pressures and leaking volumes led to high post-void residuals (PVR) and poor bladder leaking flow rate post SCI (Table 2). Bladder intravoid intervals (end of previous micturition until threshold pressure) showed significant interval time decreases post SCI (Table 2). Bladder capacity was evaluated by weighting expressed urine at morning care and at the end of each awake cystometry showed significant volume decreases at morning care and increases after cystometry (Figure 2f) (Table 2). Altogether, the data revealed that bladder capacity was increased after lumbosacral SCI, but showed no obstruction based on the expressed urine at the morning care.

Table 2: Urodynamic data of SCI rats before and 8 WPI in SCI rats.

Parameter	PRI	Group A	Group B	Group C	P-Value
Maximum intravesical pressure (cmH_2O)	38.1 ± 6,28	14.5± 2.98**	11.8 ± 1.5**	10.37 ± 1.64**	0.2842
Intravesical pressure threshold (cmH_2O)	14.93 ± 2.97	5.5 ± 0.5**	7.63 ± 1.02*	6.2 ± 0.85*	0.0975
Voided volume (ml)	0.44 ± 0.06	0.14 ± 0.01**	0.18 ± 0.05*	0.12 ± 0.03**	0.2919
Intravoid interval (s)	200.5 ± 39.83	62 ± 13*	54.62 ± 12.62*	62.25 ± 16.75*	0.5603
Flow/leaking rate (ml/s)	0.025 ± 0.003	0.006 ± 0.002**	0.01 ± 0.002**	0.007 ± 0.002**	0.4104
PVR (ml)	0	2.12 ± 0.097****	3.11 ± 1.15****	3 ± 0.69****	0.4707

n=4/group. Values are presented as mean ± SEM. P< 0.05 indicates statistical significance difference. P-value represents the significance difference among SCI group means. **** P<0.0001, *** P<0.0005, ** P<0.005, * P<0.05. Statistical significance difference between the SCI vs PRI (Two-way ANOVA). PRI; pre-SCI, WPI; weeks post SCI, PRV; post-void residual urine.

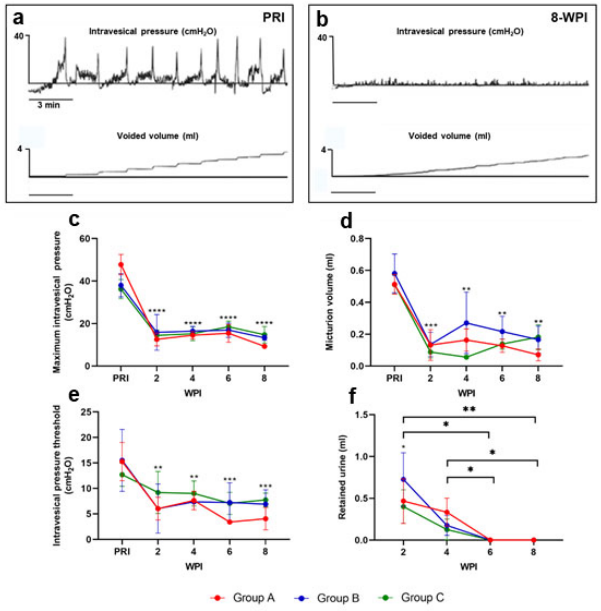

Figure 2: Effects of spinal cord injury on bladder activity and urodynamic parameters. Recordings were obtained in the unanesthetized state. Representative maximum intravesical pressure and voided volume traces in rats **(a)** pre-SCI and **(b)** 8 weeks post SCI. Bar graphs represent the cytometric parameters from SCI rats at 2, 4, 6 and 8 weeks post SCI in comparison to levels pre SCI. Parameters: **(c)** Maximum intravesical pressure, **(d)** Voided volume, **(e)** Intravesical pressure threshold, and **(f)** Weight of urine after bladder expression in the morning. Data represent mean ± S.E.M. n = 4/group. P<0.05 indicates statistical significance difference. *p<0.05, **p<0.01, ***p<0.005, ****p<0.0001. Two-way ANOVA with geisser greenhaus correction was applied to evaluate the significance difference between the SCI groups vs PRI data in each time point. SCI: Spinal Cord Injury; PRI: Pre SCI; WPI: Weeks Post SCI.

Lumbosacral SCI led to a mild locomotor function impairment

Locomotor function was measured by open-field locomotor BBB score and Multivariate gait analysis at different time points pre and post SCI. No irregularities were seen pre SCI. On day 1 post SCI, all rats exhibited a locomotor dysfunction with consistent BBB scores of 8.7±1.0 (Figure 3a). Locomotion steadily improved thereafter and plateaued at averaged scores of 14 around 2 weeks post-SCI. By two weeks post-SCI, all SCI animals achieved weight-supported stepping with hind-limbs and forelimbs (BBB scores above 11) and were able to complete Catwalk analysis. Multivariate gait analysis performed weekly started at two weeks post-SCI and included static parameters to determine changes in the placement and positioning of the paws and limbs. To objectively quantify the

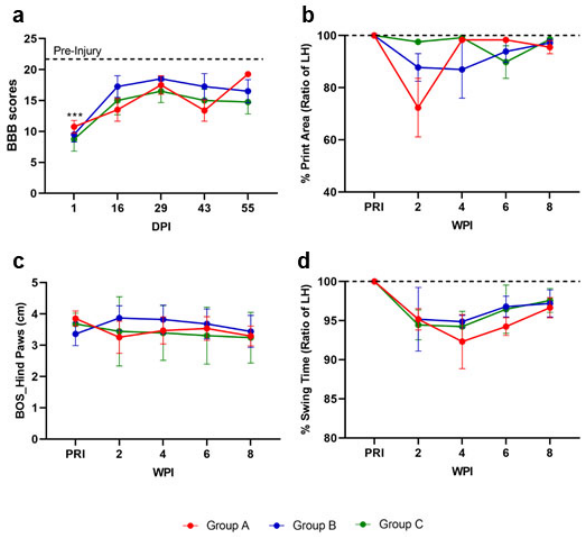

Figure 3: Locomotor analysis of rats pre and post SCI by BBB score and catwalk analysis. Graphs present **(a)** BBB score, **(b)** print area, **(c)** base of support in hind paws, and **d)** swing time. n=4/group. P<0.05 indicates statistical significance difference. *p<0.05, **p<0.01, ***p<0.005, ****p<0.0001. Two-way ANOVA with geisser greenhaus correction was applied to evaluate the significance between the SCI groups vs PRI data in each time point. BOS: Base of Support; SCI: Spinal Cord Injury, PRI: Pre SCI; DPI: Days Post SCI; WPI: Weeks Post SCI.

locomotor capacity in intact and SCI rats, the most reliable and common parameters were measured [16], including print area (Figure 3b), base of support (BOS) (Figure 3c) and swing time (Figure 3d) in the hind limbs. The results showed a mild hind limb dysfunction in all SCI animals. All assessed parameters showed a subsequent continuous recovery until 8-week post-SCI. Altogether, mild locomotor function impairment was seen in all injured rats post lumbosacral SCI, irrespective of lesion type and severity.

Underactive bladder underwent severe atrophy after lumbosacral injury

The region of interest for the histological analysis was the central bladder body. Detailed results of the histological staining are provided in Table 3 and apply again to all SCI rats, irrespective of injury type and severity.

Masson's Goldner trichrome staining to analyze structural bladder wall preservation (Figure 4A) depicted thickened bladder walls post SCI with averaging 2-fold increases (Figure 4A, a), urothelial thickness increases (Figure 4A, b) and decreased amounts of detrusor muscle (Figure 4A, c). Lumbosacral SCI also led to an increase collagen content, decreasing the ratio of type I to type III (Herovici staining, Figure 4B, a-b) (see Table 3). Further remodelling post SCI was seen in the changes in elastic fiber properties in the ECM. Elastic fibers were thinner and reduced in numbers, demonstrating a reduction in the elasticity in the bladder of SCI rats (Figure 4B arrows).

Table 3: Bladder histology data of control and SCI rats.

Parameter	Control	Group A	Group B	Group C	P value
Bladder tickness (µm)	1073 ± 10.89	2039 ± 117.7***	1852 ± 121.7***	1823 ± 193.4**	0.6144
Urothelium tickness (µm)	25.22 ± 3.25	65.84 ± 10.69**	54.63 ± 9.42*	58.2 ± 8.73*	0.9460
% MT	51.65 ± 5.33	44.09 ± 5.12	41.12 ± 2.10	34.34 ± 2.46*	0.1908
CT/MT	1.11 ± 0.09	1.56 ± 0.30	1.28 ± 0.07	1.63 ± 0.12*	0.5091
Collagen III/I	0.69 ± 0.06	1.26 ± 0.16*	1.25 ± 0.08*	0.94 ± 0.03*	0.1112

n=4/group. Values are presented as mean ± SEM. P< 0.05 indicates statistical significance difference. P-value represents the significance difference among SCI group means. *** P<0.0005, ** P<0.005, * P<0.05. Statistical significance difference between the SCI vs PRI (Two-way ANOVA). SCI; spinal cord injury, MT; muscle tissue, CT; connective tissue.

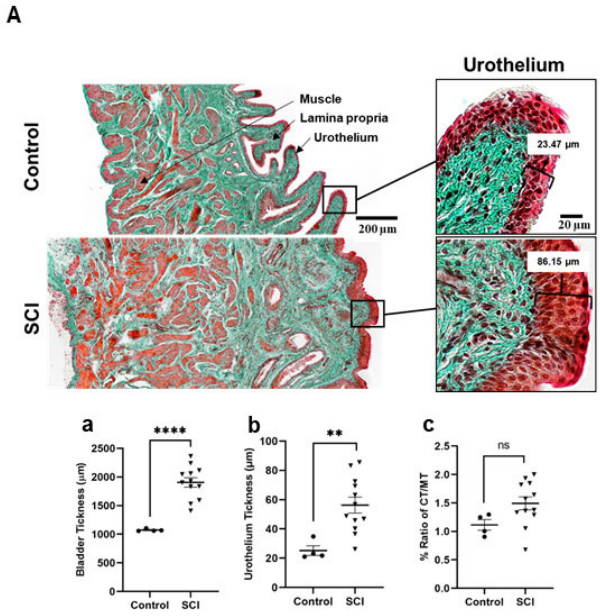

Figure 4A: Histologic analysis of the bladder body by H&E staining and Masson-Goldner trichrome staining showing marked thickening of the urothelium at 8 weeks after SCI compared with the bladder of the control group. Magnification 20x. Graphs represent **(a)** the quantified bladder wall layers, **(b)** urothelium thickness, **(c)** ratio of muscle tissue, showing the differences from control to post SCI.

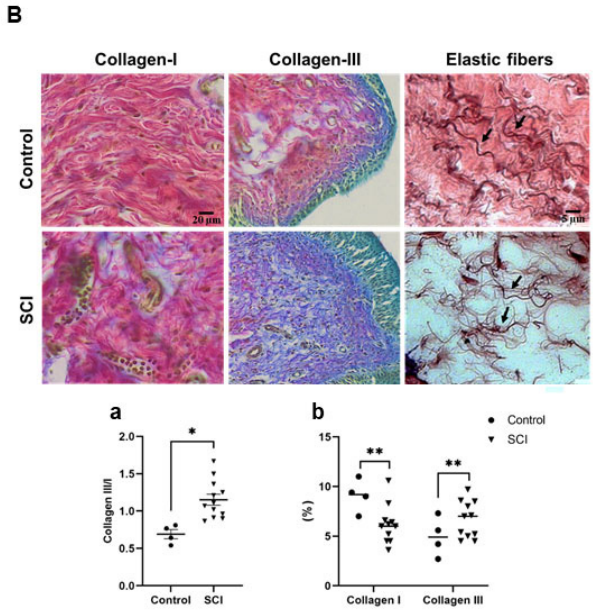

Figure 4B: Histological sections stained with H&E and Herovici to visualize collagen type I in red and type III in blue and Orcein staining to visualize the elastic fibers (arrows) in bladder of control and SCI rats. Graphs **(a-b)** showing an increase in the ratio and content of collagen III to collagen I in rat post SCI compare to control, respectively. Data represent mean ± S.E.M. P<0.05 indicates statistical significance difference. *p<0.05, **p<0.01, ***p<0.005, ****p<0.0001 (Two-way ANOVA). SCI: Spinal Cord Injury; UT: Urothelium Tissue; CT: Connective Tissue; MT: Muscle Tissue; Coll-I: Collagen Type I; Coll-III: Collagen Type III; H&E: Hematoxylin and Eosin.

Discussion

In humans, the bladder reflex arc is located in S2-S4, the terminal segments of the adult spinal cord, and lies at the level of T12/L1 in most adults [17,18]. Clinically, bladder dysfunction after thoracolumbar SCIs may include loss of voluntary micturition, impaired urethral closure, and an areflexia bladder [19-21]. However, SCIs at the terminal segments of the spinal cord are complex, and the relative contribution of these lesions to the central and peripheral parts of the nervous system may vary from patient to patient. Therefore, it can be difficult to predict how limiting an injury may be given the different types of bladder dysfunction.

Since the animal models to study thoracolumbar injuries have been relatively sparse, in the present study, we investigated the bladder and locomotor functions following contusive SCI to the T13/L1junction, L1 vertebral level and L1/L2 junction with the L5 to S2 spinal cord segments in a rat model. These levels were selected to include primarily the L6 and S1 segments, which contain the preganglionic parasympathetic neurons innervating the detrusor muscle and the somatic motoneurons innervating the external urethral sphincter (EUS) [22,23].

High resolution μCT imaging of the injured spinal cords was performed, and lesion characteristics were analysed semiautomatically at the epicentral foci and also extended rostro-caudal. Based on the anatomy of lumbosacral spinal cord segments, the spinal cord in this area is cone-shaped and the size of the spinal segments becomes smaller in the region of the cauda equina. At that point, group A included thoracolumbar junction lesion that had the shortest defect length and volume. Group B included the L1 vertebral lesion had the largest cyst volume, and group C included L1/L2 junction lesions and had the most caudal injuries with the longest defect lengths and volumes. Lesions at lumbar spine may spare a critical portion of white and gray matter containing axons and sensory and motoneurons located in the intermediate lateral and ventral horn of the respective segments, mediating bladder function. To know the functional deficits among the three groups with the varying lesion lengths and widths and degrees of white and gray matter sparing, bladder and motor outcomes were analyzed.

Since the type of resulting functional disturbance depends on the nature and extent of nerve injury, the urodynamic assessment among SCI rats with different lesion areas needs a careful examination. In the present rat model, a consistent functional deficit of the bladder was observed in the three different injury groups, although contusion resulted in varying damage to the parenchyma. Our cystometric data showed a significant decrease in bladder strength combined with low leaking volumes and high retained urine compared to data pre SCI. This is in line with clinical observations, where any lesion at the lumbosacral spine causes some degree of voiding deficiency [24]. Based on the neural mechanism of micturition, low intravesical pressures, which indicates an hypocontractile detrusor, resulted most likely from the damage to parasympathetic efferent pathways in lumbosacral spinal cord. Moreover, the low volume of retained urine during morning bladder expression may indicate the damage to the motoneurons in Onuf's nucleus in the lumbosacral spinal cord that fosters neurogenic EUS closure [4,18]. The other finding of the urodynamic analysis was the high PVR without changes in bladder pressure indicating high compliances post SCI and can be associated with an increased bladder capacity in conditions such as underactive or flaccid bladder. The preservation of sympathetic neurons in L1-L2 spinal cord innervating the bladder neck may explain the paradoxical symptomatology of both leaking across the urethra and the inability to empty the bladder. Based on urodynamic finding, the disruption of bladder function is not due to differences in lesion size nor to sparing of different portions of white and gray matter at the lumbosacral level.

The lumbosacral spinal cord contains also critical motor centers, including the central pattern generator (CPG) and the tibial nerve innervating the gastrocnemius and gluteus maximus muscles [25]. The BBB score locomotor scale was used to define the consistency of injury outcomes among individual SCI rats. Previous studies have reported mild locomotor deficits and relatively little changes of the BBB locomotor scores after contusion injury at vertebral level T13 [26,27]. The BBB scores revealed similar mild impairments in trunk stability and coordination in our SCI rat collective, again similar findings for all lesion groups. The catwalk findings indicated that rats with lumbosacral lesions are able to walk with restrains in complete coordination and a disability of complete paw placement. However, this infirmity was almost totally recovered during eight weeks post SCI. The deficits in locomotor function were similar among all three injury groups. This mild locomotor deficit suggests some but not extensive sharing of neurons that control the two functional neural networks (locomotor and bladder motoneurons). The results obtained in this rat model reflect the deficits described in patients with lumbosacral SCI, who may experience some degree of function loss in the hips and legs but will most likely be able to walk [28]. In our animal model, several histological stainings were done to compare functional results to structural remodeling. Results showed an alteration in the urothelium of the bladder of all SCI rats. No significant difference in structural bladder changes were seen between the 3 distinct lesion groups. A significant increase in the bladder wall and urothelial thickness were seen in SCI rats. These findings are consistent with previous clinical observations that hypothesized that SCI and the resulting lack of trophic action on the urothelium might lead to a cascade of events involving urothelial proliferation, differentiation, and apoptosis [29-31]. Mucosal denervation, cell adhesion molecules, secretory immunoglobulin (IgA), growth factors, nitric oxide synthase

(NOS), and cytokines could play a complex and interactive role in the development of the denervation-induced changes in urothelial structure and function; these cellular changes could eventually lead to increased susceptibility of the vesical urothelium to urinary tract infection, and the present animal model may be a suitable subject to determine the mechanisms.

Regarding the detrusor muscle layer, a decrease in the ratio of detrusor muscle layer to the whole bladder wall thickness and connective tissue amount was observed in SCI rats. Relevant to this alteration, neurogenic atrophy of detrusor muscle is described in chronic SCI patients [32]. In addition, to determine the increase in collagen contents of the rat SCI bladder, investigations of the correlations between collagen types III and I showed a dominance in collagen III in SCI rats. The modest amounts of collagen III were observed in the lamina propria, parallel to the urothelium. The linearized fibrils conformation of the collagen III in the submucosal area indicated more stress in this area, maybe due to the large post-void residual volumes and/or acontractile bladder pathology. This would be accounted for the ability of the bladder to accommodate large changes in volume. Additionally, it has been shown that the low bladder pressure causes a loss of elasticity in the bladder tissue [33]. Also, the changes in elastic fibers by decreasing their number and length demonstrate nonreversible dilation of the acontractile bladder in SCI rats.

These findings align with the urodynamic finding of acontractile bladders with low intravesical pressures. Furthermore, our rat data matches clinical observations, where an increase in size of the acontractile bladder with a progressive structural remodeling, widened ECM with extensive collagen deposition, and axonal degeneration is described as the major features of neurogenic areflexia bladder [29,34].

Concluding Remarks

All collected data and conclusions highlight the multifactorial nature of neurogenic bladder dysfunction (NBD) following lumbosacral SCI. This new rat model closely reproduced the main aspects of human NBD following lesions to conus medullaris or cauda equine and provided deep insight into the mechanisms underlying the pathogenesis of this complex condition. Finally, a standardized and well-described neurological animal model is available to test new strategies to tackle the NBD condition and may ultimately help to improve the quality of life of affected patients.

List of Abbreviations

SCI: Spinal Cord Injury; NBD: Neurogenic Bladder Dysfunction; UAB: Underactive Bladder; EUS: External Urethral Sphincter; VRA: Ventral Root Avulsion; LCS: Lumbar Canal Stenosis; PVR: Post-Void Residuals; Pves: Intravesical Pressure; BBB: Basso, Beattie And Bresnahan; BOS: Base Of Support; CPG: Central Pattern Generator; LH: Left Hind; ECM: Extracellular Matrix; IgA: Secretory Immunoglobulin; NOS: Nitric Oxide Synthase.

Ethics Approval and Consent to Participate

This animal study was approved by the Federal Ministry of the Republic of Austria, Section Education, Science and Research under the animal ethical approval number BMB WF-6C.019/0015-V/3b/2019.

Consent for Publication

Not applicable.

Availability of Data and Materials

The datasets used and/or analyzed during the current study are available from the corresponding author on reasonable request.

Competing Interests

The authors declare that they have no competing interests.

Funding

This work was supported by grants from the Paracelsus Medical University Forschungsförderungsfond (FFF) (R-19 / 03 / 119-AFR).

Authors' Contributions

BA designed the study, conducted the animal work, analyzed and interpreted the urological data sets and was a major contributor in writing the manuscript. KR conducted the animal work, processed the tissues and performed histological/immunohistochemical analyses. SB was involved in the study design, interpretation of urological data, correlation to clinical settings and writing the manuscript. LL was involved in designing the study, analyzing the urological data and correlation to clinical settings. PH and DH analyzed and interpreted the µ-CT data sets and contributed to writing the manuscript. LA was involved in the design, general data analysis and manuscript writing process. EK designed the study, contributed to the animal work and data generation and interpretation, and was a major contributor in writing the manuscript. All authors read and approved the final manuscript.

Acknowledgements

The authors wish to thank Professor Sébastien Couillard-Després (Department of Experimental Neuroregeneration, Spinal Cord Injury and Tissue Regeneration Center Salzburg, Austria) for his valuable advice and Dr. Andrea Wagner and the Spinal Cord Injury and Tissue Regeneration Center Salzburg Core Facilities Imaging and Histology for excellent technical support.

References

1. Spinal cord injury facts and figures at a glance. 2014. J Spinal Cord Med, 37: 117-8.

2. Goetz LL, Cardenas DD, Kennelly M, Lee B, Linsenmeyer T, Moser C, et al. International spinal cord injury urinary tract infection basic data set. Spinal Cord. 2013 Sep;51(9):700-4.

3. Böthig R, Tiburtius C, Schöps W, Zellner M, Balzer O, Kowald B, et al. Urinary bladder cancer as a late sequela of traumatic spinal cord injury. Military Medical Research. 2021 Dec;8(1):29.

4. de Groat WC, Griffiths D, Yoshimura N. Neural control of the lower urinary tract. Comprehensive Physiology. 2015 Jan;5(1):327-96.

5. Blaivas JG. The neurophysiology of micturition: a clinical study of 550 patients. The Journal of Urology. 1982 May 1;127(5):958-63.

6. Perlow DL, Diokno AC. Predicting lower urinary tract dysfunctions in patients with spinal cord injury. Urology. 1981 Nov 1;18(5):531-5.

7. Weng YC, Chin SC, Wu YY, Kuo HC. Clinical, neuroimaging, and nerve conduction characteristics of spontaneous Conus Medullaris infarction. BMC Neurology. 2019 Dec;19(1):1-9.

8. Krucoff MO, Gramer R, Lott D, Kale E, Yadav AP, Abd-El-Barr MM, et al. Spinal cord stimulation and rehabilitation in an individual with chronic complete L1 paraplegia due to a conus medullaris injury: motor and functional outcomes at 18 months. Spinal Cord Series and Cases. 2020 Oct 16;6(1):1-9.

9. Chang HH, Havton LA. A ventral root avulsion injury model for neurogenic underactive bladder studies. Experimental Neurology. 2016 Nov 1;285:190-6.

10. Sekido N, Jyoraku A, Okada H, Wakamatsu D, Matsuya H, Nishiyama H. A novel animal model of underactive bladder: analysis of lower urinary tract function in a rat lumbar canal stenosis model. Neurourology and Urodynamics. 2012 Sep;31(7):1190-6.

11. Hannan JL, Powers SA, Wang VM, Castiglione F, Hedlund P, Bivalacqua TJ. Impaired contraction and decreased detrusor innervation in a female rat model of pelvic neuropraxia. International Urogynecology Journal. 2017 Jul;28(7):1049-56.

12. Schneider MP, Hughes FM, Engmann AK, Purves JT, Kasper H, Tedaldi M, Spruill LS, Gullo M, Schwab ME, Kessler TM. A novel urodynamic model for lower urinary tract assessment in awake rats. BJU International. 2015 Jan 18;115:8-15.

13. Foditsch EE, Roider K, Sartori AM, Kessler TM, Kayastha SR, Aigner L, et al. Cystometric and external urethral sphincter measurements in awake rats with implanted catheter and electrodes allowing for repeated measurements. JoVE (Journal of Visualized Experiments). 2018 Jan 30(131):e56506.

14. Basso DM, Beattie MS, Bresnahan JC. A sensitive and reliable locomotor rating scale for open field testing in rats. Journal of Neurotrauma. 1995 Feb;12(1):1-21.

15. Meijering EH, Niessen WJ, Viergever MA. Quantitative evaluation of convolution-based methods for medical image interpolation. Medical Image Analysis. 2001 Jun 1;5(2):111-26.

16. Harrigan ME, Filous AR, Tosolini AP, Morris R, Schwab JM, Arnold WD. Assessing rat forelimb and hindlimb motor unit connectivity as objective and robust biomarkers of spinal motor neuron function. Scientific Reports. 2019 Nov 13;9(1):1-4.

17. Ganapathy MK, Reddy V, Tadi P. Neuroanatomy, spinal cord morphology. In: StatPearls. Florida: StatPearls Publishing. 2020.

18. Fowler CJ, Griffiths D, De Groat WC. The neural control of micturition. Nature Reviews Neuroscience. 2008 Jun;9(6):453-66.

19. Taylor III JA, Kuchel GA. Detrusor underactivity: clinical features and pathogenesis of an underdiagnosed geriatric condition. Journal of the American Geriatrics Society. 2006 Dec;54(12):1920-32.

20. Hellström P, Kortelainen P, Kontturi M. Late urodynamic findings after surgery for cauda equina syndrome caused by a prolapsed lumbar intervertebral disk. The Journal of Urology. 1986 Feb 1;135(2):308-12.

21. Bradley WE, Andersen JT. Neuromuscular dysfunction of the lower urinary tract in patients with lesions of the cauda equina and conus medullaris. The Journal of Urology. 1976 Nov 1;116(5):620-1.

22. Marson L. Identification of central nervous system neurons that innervate the bladder body, bladder base, or external urethral sphincter of female rats: a transneuronal tracing study using pseudorabies virus. Journal of Comparative Neurology. 1997 Dec 29;389(4):584-602.

23. McKenna KE, Nadelhaft I. The organization of the pudendal nerve in the male and female rat. Journal of Comparative Neurology. 1986 Jun 22;248(4):532-49.

24. Sakakibara R, Uchiyama T, Yamaguchi C, Yamamoto T, Ito T, Liu Z, et al. Urinary retention due to an isolated sacral root injury caused by sacral fracture. Spinal Cord. 2007 Dec;45(12):790-2.

25. Nicolopoulos-Stournaras S, Iles JF. Motor neuron columns in the lumbar spinal cord of the rat. Journal of Comparative Neurology. 1983 Jun 10;217(1):75-85.

26. Edgerton VR, Roy RR, Hodgson JA, Prober RJ, De Guzman CP, De Leon R. Potential of adult mammalian lumbosacral spinal cord to execute and acquire improved locomotion in the absence of supraspinal input. Journal of Neurotrauma. 1992 Mar 1;9:S119-28.

27. Sherrington CS. Flexion-reflex of the limb, crossed extension-reflex, and reflex stepping and standing. The Journal of physiology. 1910 Apr 26;40(1-2):28-121.

28. Chen SL, Huang YH, Wei TY, Huang KM, Ho SH, Bih LI. Motor and bladder dysfunctions in patients with vertebral fractures at the thoracolumbar junction. European Spine Journal. 2012 May;21(5):844-9.

29. Van Velzen D, Krishnan KR, Parsons KF, Soni BM, Howard CV, Fraser MH, et al. Vesical urothelium proliferation in spinal cord injured persons: an immunohistochemical study of PCNA and MIB. 1 labelling. Spinal Cord. 1995 Sep;33(9):523-9.

30. Dewulf K, Weyne E, Gevaert T, Deruyver Y, Voets T, De Ridder D,

et al. Functional and Molecular Characterization of the Bilateral Pelvic Nerve Crush Injury Rat Model for Neurogenic Detrusor Underactivity. BJU Int. 2018;123(5A):E86-96.

31. Kim SJ, Kim J, Na YG, Kim KH. Irreversible bladder remodeling induced by fibrosis. International Neurourology Journal. 2021 May;25(Suppl 1):S3-7.

32. Przydacz M, Chlosta P, Corcos J. Recommendations for urological follow-up of patients with neurogenic bladder secondary to spinal cord injury. International Urology and Nephrology. 2018 Jun;50(6):1005-16.

33. Landau EH, Jayanthi VR, Churchill BM, Shapiro E, Gilmour RF, Khoury AE, Macarak EJ, Mclorie GA, Steckler RE, Kogan BA. Loss of elasticity in dysfunctional bladders: urodynamic and histochemical correlation. The Journal of urology. 1994 Aug 1;152(2):702-5.

34. Fusco F, Creta M, De Nunzio C, Iacovelli V, Mangiapia F, Li Marzi V, et al. Progressive bladder remodeling due to bladder outlet obstruction: a systematic review of morphological and molecular evidences in humans. BMC Urology. 2018 Dec;18(1):15.